ELSEVIER

Journal of Molecular Catalysis A: Chemical 193 (2003) 217–226

JOURNAL OF MOLECULAR CATALYSIS A: CHEMICAL

www.elsevier.com/locate/molcata

Effect of sulfation on the photoactivity of TiO_2 sol–gel derived catalysts

R. Gómez [a,*], T. López [a,1], E. Ortiz-Islas [a], J. Navarrete [b], E. Sánchez [c], F. Tzompanztzi [c], X. Bokhimi [d]

[a] *Departmento de Química, Universidad Autónoma Metropolitana-Iztapalapa, P.O. Box 55-534, México 09340 D.F., Mexico*
[b] *Instituto Mexicano del Petróleo, Gerencia de Catalisis, Eje Central Lazaro Cardenas 152, México 07000 D.F., Mexico*
[c] *Universidad Autonóma de Nuevo León, Pedro de Alba s/n San Nicolás de los Garza N.L., Mexico*
[d] *IFUNAM, C.U. México 10000 D.F., Mexico*

Received 30 April 2002; accepted 6 August 2002

Abstract

Titania and sulfated-titania were prepared by the sol–gel method using titanium alkoxide as titania precursor. BET specific surface areas on samples calcined at 600 °C were 57 and 62 m^2/g for titania and sulfated-titania, respectively. FTIR spectra of sulfated samples show the 1360–1370 cm^{-1} absorption band assigned to S=O vibrations. Moreover, by means of FTIR-pyridine absorption the strength of the sulfate bonded on the TiO_2 surface was studied. Pyridine absorption bands assigned to Lewis and Bronsted acidic sites were identified on sulfated TiO_2. A diminution of the band gap (E_g) by effect of sulfation was observed by UV-Vis spectroscopy. X-ray diffraction patterns show that sulfate ions stabilize the anatase phase. The photoactivity of the samples determined in the 2,4-dinitroaniline decomposition was found to be higher in sulfated samples. A model is proposed, in which the sulfate anchored to the titania surface acts as an electron trap during photo activation leading to an enhancement of activity.

Keywords: Titania sol–gel; Titania-sulfated; Titania band gap; Titania-sulfated X-ray diffraction; Titania-sulfated photoactivity; Titania-sulfated acidity

1. Introduction

The industrial treatment of polluted industrial wastewater to eliminate toxic compounds is one the most important subjects under study around the world. Biological digestion, chemical oxidation or absorption of pollutants in activated carbon, have been the traditional methods used in industrial water purification units. However, these treatments are not as efficient as desired. The active micro-organisms are restricted by the operating conditions, strict pH and temperature control. Chemical oxidation is not complete for many organic compounds, and the absorption of toxic substances transfers the pollutants to the absorbant [1,2]. Photodegradation using semiconductors in aqueous solutions appears to be an alternative method for wastewater treatment [3]. The advantages of the method are that the semiconductor remains as a solid after reaction and it can be separated from the reactant medium by filtering. Semiconductors can react at room temperature, making the overall process economical. Most studies related to the photocatalytic

* Corresponding author.
E-mail address: gomr@xanum.uam.mx (R. Gómez).
[1] Co-corresponding author.

1381-1169/02/$ – see front matter
PII: S1381-1169(02)00473-9

degradation of organic compounds have been carried out with titania in aqueous reactant medium. A large list of organic compounds among them: chlorine-compounds [4,5], phenols [6–10], cresols [11], alcohols [12,13], surfactants, pesticides and dyes have seen decomposed successfully [1].

The photocatalytic activity of titania as semiconductor has been illustrated in recent reviews by Hermann [1]. According to Hermann, the photo efficiency is attributed to the electron-hole pair recombination occurring after irradiation. Any attempt to trap the electrons formed by the photonic excitation, results in a greater photoactivity. In this way, it has been reported that Ag [14], AgPt [15], Pt [16,17] or Pd [18] deposited on titania can improve the photoactivity. The metal function is attributed to an electron source, for example, Ag can reduce $PtCl_6^{2-}$ ions on its surface.

Recent studies show that SO_4^{2-} ions can be anchored on the surface of TiO_2, developing strong acidity. The sulfate ion forms S=O and O–S–O bonds in bulk and surface, creating unbalanced charge on Ti and vacancies and defects in the titania network [19–21].

Titania synthesized by the sol–gel process seems be an appropriate method to obtain TiO_2 [22–25], Pt/TiO_2 [26], Fe_2O_3/TiO_2 [27,28], TiO_2–SiO_2 [29] or TiO_2–ZrO_2 [30] catalysts with photoactivity properties. When TiO_2 [31] or TiO_2–SiO_2 mixed oxides [32,33] were prepared and sulfated, a high SO_4^{2-} ion concentration anchored to the TiO_2 was observed. Additionally, an advantage of synthesizing TiO_2 by gelling titanium alkoxides, is that in such preparations the specific surface areas, titania crystallite size, crystalline titania phases [34–37], and band gap energy [38,39] of TiO_2 can be controlled. When metals were supported on TiO_2 sol–gel preparations, improved selectivity was reported for the phenylacetylene hydrogenation [40] and high resistance to sintering was reported for carbon monoxide oxidation and NO reduction [41–43]. Overall, the final properties of sol–gel catalysts can be controlled, mainly by varying the hydrolysis pH and the relative water/alkoxide ratio [44,45].

In the present work with the aim to improve the photocatalytic properties of TiO_2, we prepared sol–gel titania to which sulfate ions were anchored on the surface. The textural properties of the solid was characterized by nitrogen adsorption isotherms, UV-Vis spectroscopy, FTIR-pyridine absorption, XRD spectroscopy, and by their photoactivity in the 2,4-dinitroaniline decomposition.

2. Experimental

2.1. Catalyst preparation

The preparation of the TiO_2 reference catalyst was as follows: to a reflux glass system containing 200 ml of *tert*-butyl alcohol (Baker 99.9%) and 200 ml of double distilled water, ammonium hydroxide (Baker 29 vol.% in water) was added to reach pH 9. Next, under refluxing and constant stirring 84.5 ml of titanium tetra-*n*-butoxide (Aldrich 98%) were added drop wise and the solution was maintained for 24 h. Subsequently, the solution gelled. This was followed by drying at 100 °C for 12 h in an oven (fresh sample). Afterwards, the sample was calcined at 600 °C in a furnace for 3 h in flowing air (3.6 l/h).

2.1.1. Sulfated TiO_2

The TiO_2 reference solid was sulfated by impregnating 1.0 g of the dried support (fresh sample) with 5 ml of a solution of ammonium sulfate (1N) and maintained under stirring for 3 h. Afterwards the excess of water was evaporated until dryness and then calcined at 600 °C in a furnace for 3 h in flowing air (3.6 l/h).

2.2. Specific surface area

The specific surface areas of the samples calcined at 600 °C were obtained using a Micromeritics Sorptometer ASAP 2000. The specific areas were calculated from the nitrogen isotherms using the BET method and the mean pore diameter was calculated from the BJH method.

2.3. Sulfur analysis

The sulfur content of the samples calcined at 600 °C was determined in a Model SC 444 LECO S analyser by calcining the solids at 1300 °C, followed by gas analysis in a S detector (UV-Vis).

2.4. FTIR-spectroscopy

Infrared spectroscopy was performed using a Nicolet 710 spectrophotometer. The sample was pressed

into a thin self-supported wafer and placed in the infrared cell, which allows "in situ" treatments. After evacuation at 450 °C for 2 h, the cell was cooled to room temperature. The evacuated samples were then contacted with pyridine from a capillary tube fractured in the cell. The excess of pyridine was then eliminated by evacuation of the cell. Under vacuum the spectra of adsorbed pyridine were recorded at different desorption temperatures.

2.5. UV-Vis absorption spectra

The UV-Vis absorption spectra of the samples were obtained with a Cary-III spectrophotometer equipped with an integrator sphere for diffuse reflectance studies. MgO (100%) was used as reflectance reference.

2.6. X-ray diffraction studies

X-ray spectra were obtained with a Siemens D-500 diffractometer using Cu Kα radiation. The spectra were obtained from specimens prepared by packing sample powder into a glass holder. The intensity of the signals was measured by step scanning in the 2θ range between 10 and 110° with a step of 0.02° and a measuring time of 2 s per point. Diffraction peak profiles were modeled with a pseudo-Voight function that used the average crystallite size as a fitting parameter [46,47]. The standard deviations are given in parenthesis.

2.7. Photocatalytic activity

Photoactivity measurements were carried out at room temperature as follows: in a flask containing an aqueous solution at 30 ppm of 2,4-dinitroaniline, 100 mg of catalyst were added under stirring. Then, the solution was irradiated in a closed box with a UV lamp Black-Ray model XX-15L, which emits a radiation $\lambda = 254$ nm and an intensity of 1600 μW/cm^2. The light received by the vessel was 1560 μW/cm^2. The reaction rate was followed with a UV-Vis spectrophotometer Hewlett-Packard model 8452 equipped with a diode array as detector. The concentration of the 2,4-dinitroaniline was calculated from the intensity of the absorption band at 346 nm. Before the activity test of TiO_2 and sulfated-TiO_2 sol–gel catalysts, first the solution containing the 2,4-dinitroaniline without catalysts was irradiated, and second, the solution containing the reactant and the catalysts was put in contact without irradiation. In both cases, any decomposition of the 2,4-dinitroaniline was observed.

3. Results

3.1. Specific surface areas

The BET specific surface areas of the samples calcined at 600 °C were 57 and 62 m^2/g for TiO_2 and sulfated-titania, respectively. The mean pore size calculated from BET isotherms were 11.9 and 15.0 nm, respectively. The sulfur content of the sulfated-titania was 0.59 wt.%.

3.2. FTIR-spectroscopy

In order to identify the sulfate S=O species anchored to TiO_2, we followed the characteristic FTIR absorption band around 1380–1360 cm^{-1} which are assigned to S=O and O=S=O stretching vibrations [19]. The FTIR spectra of sulfated-titania calcined at 600 °C and exposed to ambient for 24 h is shown in Fig. 1. Thermal treatment was applied under vacuum and the evolution of the 1360 cm^{-1} band is shown as a function of the temperature. This band corresponds to $(TiO)_3$–S=O and to $(TiO)_2$–SO_2 asymmetric vibrations [48–51].We can see that the S=O band appears around 1320 cm^{-1} in the sample observed after ambient exposure. This band is shifted to 1369 cm^{-1} when the temperature of the sample reaches 400 °C. In our case, because the sample was exposed to wet atmosphere, the S=O species coordinate water and hence the S=O band appears at lower frequency as an S–O vibration band [52,53]. When the temperature of the sample was raised, the adsorbed water was eliminated and the band is then shifted to higher frequency. The phenomenon occurring during the thermal treatment is illustrated in Fig. 2. The most important fact is that in our sol–gel sulfated-titania, we still observe S=O bonds in samples thermally treated as high as 600 °C.

3.3. FTIR-pyridine absorption spectra

It has been reported that sulfation induces acidity on titania and the nature of the acidic sites can be

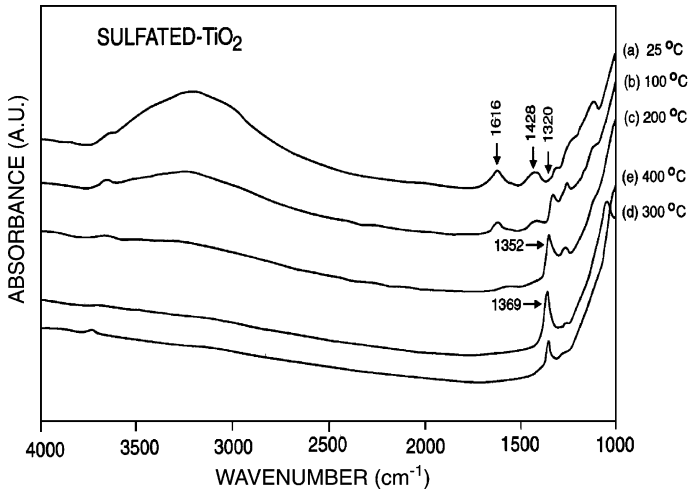

Fig. 1. FTIR spectra of sulfated-titania (600 °C) after exposure to wet atmosphere.

determined by FTIR-pyridine thermodesorption studies [19–21]. For the sample calcined at 600 °C the FTIR spectra are shown in Fig. 3. The pyridine absorption bands are observed at 1445, 1487, 1540 and 1600 cm^{-1}. They are assigned to pyridine coordinated on Lewis acidic sites and to the vibration of the pyridinic ring on Bronsted or Lewis sites. In the spectra, a broad band also can be seen at 1266 cm^{-1} related to S–O vibrations [52,53]. The bands at 1540 and 1487 decrease with temperature and practically disappear when the temperature reaches 300 °C. In contrast, the bands at 1600 and 1445 cm^{-1} can be seen even when desorption temperature reaches 400 °C.

We investigated the behavior of the1266 cm^{-1} band further. This band shifted to 1331 cm^{-1} when the pyridine desorption temperature reached 500 °C. The band is associated with S–O vibrations. Morterra et al., explains the effect on sulfated ZrO_2 assuming that bases (like pyridine) interact with the S=O modifying their electronic density [54]. When the pyridine is desorbed, the S=O bonds acquire their covalent character, and then the vibration band appears at the IR region 1344–1331 cm^{-1}. If sulfated TiO_2 is not so far of the model proposed by Morterra for sulfated ZrO_2 [54], the coordination of pyridine with S=O and its modification to S–O bonds could be explained using the same model for water coordinated in wet samples (Fig. 2).

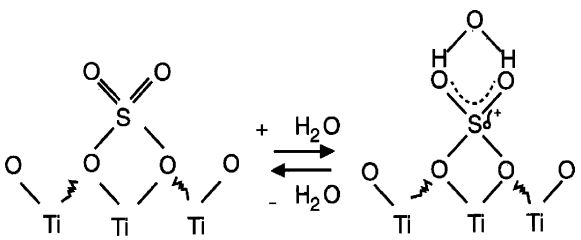

Fig. 2. Sulfated-TiO_2 model explaining the S=O and water coordinated to S=O bonds.

3.4. X-ray diffraction spectroscopy

The quantitative analysis of the crystalline phases was made from the XRD patterns using the Rietveld refinement method.

The phase concentration of the samples is listed in Table 1. In annealing the samples at 600 °C, anatase (81%) and rutile (19%) phases were observed for TiO_2, while in sulfated-titania only the anatase phase

Table 1
Band gap (E_g) and crystalline phase composition (in wt.%) of TiO_2 and sulfated-TiO_2

Catalyst	Band gap (eV)	Anatase	Rutile
TiO_2-600 °C	3.32	81 (2)	19 (2)
TiO_2-SO_4-600 °C	3.03	100 (2)	–

The value in parenthesis are the estimated standard deviations.

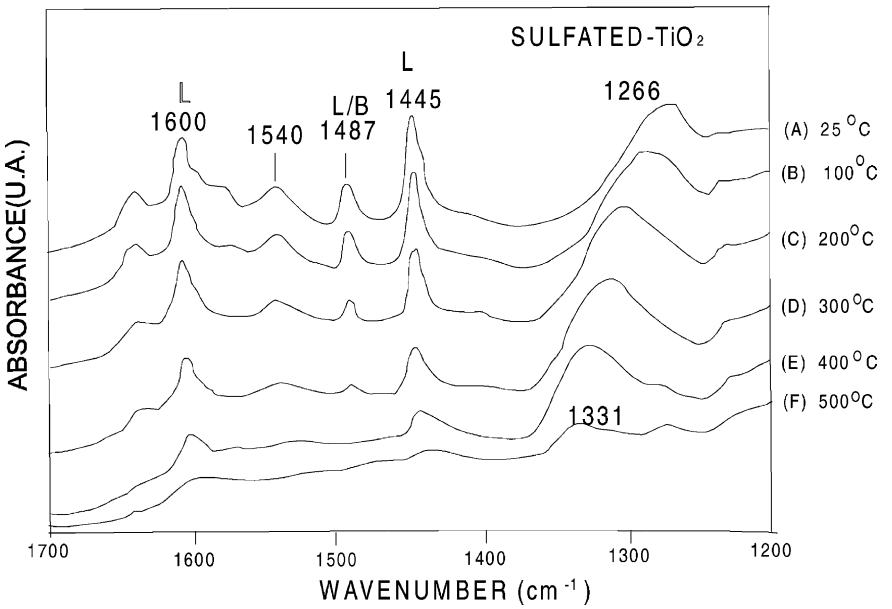

Fig. 3. FTIR-pyridine absorption spectra of sulfated-TiO_2.

was identified, i.e. sulfation has an strong effect on the relative anatase/rutile phases abundance.

The Rietveld refinement method used to evaluate the crystalline phases concentration from the XRD spectra for TiO_2 and sulfated-titania calcined is illustrated in Fig. 4. In the spectra it can be seen that in sulfated-titania, the only crystalline phase observed was anatase. Such behavior does not occur in the calcined titania reference sample, since anatase and rutile phases co-exist.

3.5. UV-Vis spectroscopy

Because of its semiconductor properties, the band gaps (E_g) of the TiO_2 and sulfated-titania were calculated using the equation $\alpha(h\upsilon) = A(h\upsilon - E_g)^{m/2}$, where α is the absorption coefficient, $h\upsilon$ the energy of the photon and $m = 1$ for a direct transition between bands. For practical purpose, E_g can be calculated from extrapolation of the straight line from the absorption curve to the abscissa (38). The corresponding experimental UV-Vis spectra are shown in Fig. 5, and the calculated E_g bands are reported in Table 1. The E_g band for the TiO_2 is of 3.32 eV, while on sulfated-titania the E_g decreases to 3.03.

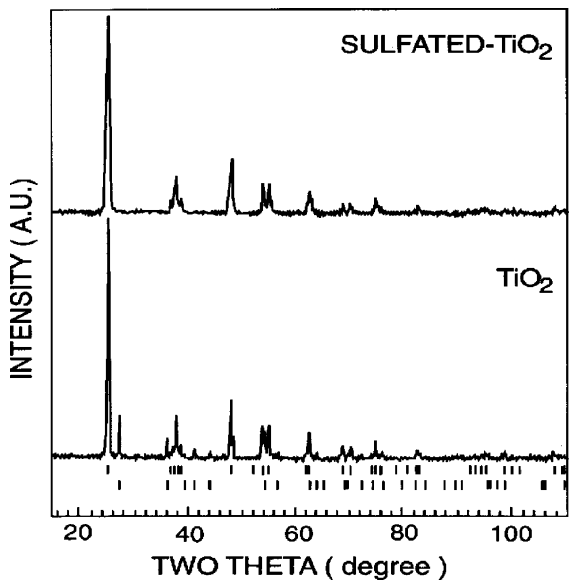

Fig. 4. XRD patterns of TiO_2 and sulfated-TiO_2 annealed at 600 °C. Upper tick marks correspond to anatase and the lower ones to rutile.

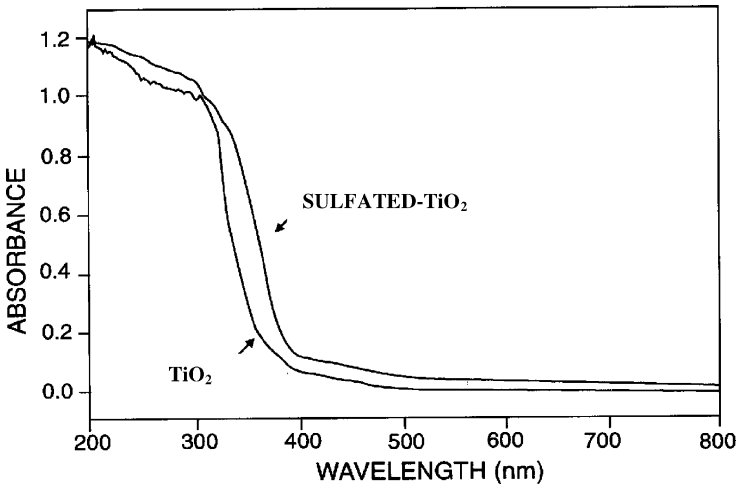

Fig. 5. UV-Vis spectra of TiO_2 and sulfated-TiO_2 calcined at 600 °C.

3.6. Photocatalytic properties

To evaluate the photoactivity of TiO_2 and sulfated-TiO_2 the decomposition of 2,4-dinitroaniline at room temperature was studied. The decomposition of the reactant as a function of time was evaluated following the UV absorption band at 346 nm. The evolution of the 2,4-dinitroaniline decomposition as a function of time is shown in Fig. 6. Kinetic parameters where obtained from the curves by application of the Langmuir–Hinselwood equation [55], for heterogeneous photocatalytic reactions, in a similar way as has been reported for Li/TiO_2 and Rb/TiO_2 sol–gel derived photocatalysts [56].

$$r = \frac{k_1 k_2 C}{1 + k_2 C}$$

This equation became linear as:

$$\frac{1}{r} = \frac{1}{k_1} + \frac{1}{k_1 k_2 C}$$

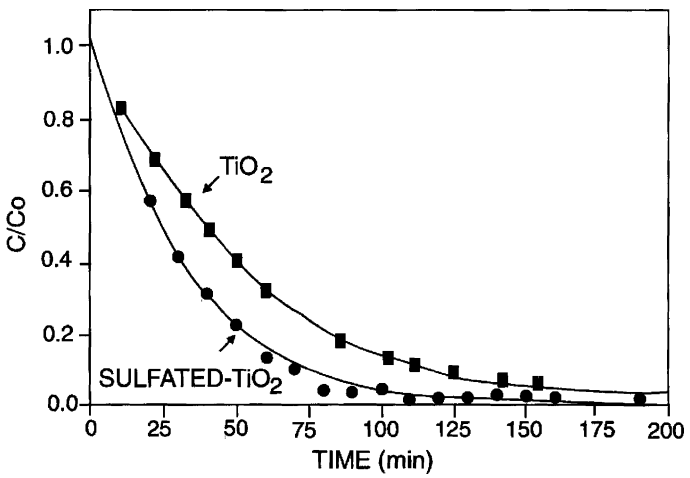

Fig. 6. Decomposition of 2,4-dinitroaniline on function of time on TiO_2 and sulfated-TiO_2 calcined at 600 °C.

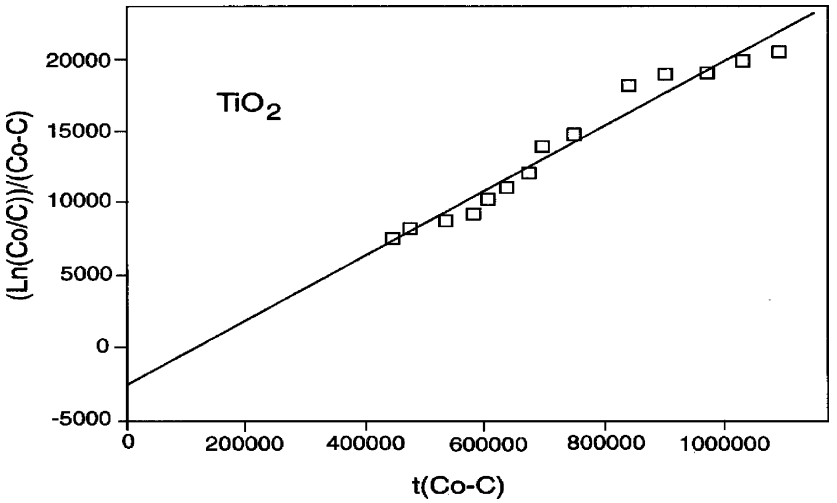

Fig. 7. Graphic presentation of Langmuir–Hinselwood model for the decomposition of 2,4-dinitroaniline on TiO_2 calcined at 600 °C.

For a batch reactor we have:

$$-\frac{V\,\mathrm{d}C}{\mathrm{d}t} = \frac{mAk_1k_2C}{1+k_2C}$$

integrating from $t = 0$ to $t = i$ and for the initial concentration C_0 to the C_i concentration, we have:

$$\frac{\ln C_0/C}{C_0 - C} = \frac{k_2 + (mAk_1k_2)t}{V(C_0 - C)}$$

and finally to estimate the time in which $C_0 = C_0/2$ we use:

$$t_{1/2} = \frac{[(0.693/k_1k_2) + (C_0/2k_1)]}{mA/V}$$

where r is the reaction rate; k_1 the apparent rate constant; k_2 the adsorption constant; m the mass of catalyst; A the adsorption sites by g/cat. and V the liquid volume.

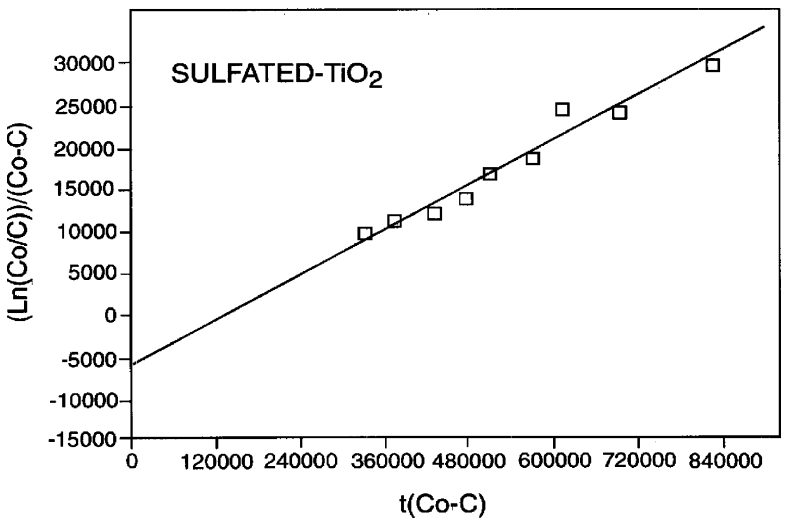

Fig. 8. Graphic presentation of Langmuir–Hinselwood model for the decomposition of 2,4-dinitroaniline on sulfated-TiO_2 calcined at 600 °C.

Table 2
Langmuir–Hinshelwood parameters and photoactivity for the 2,4-dinitroaniline decomposition on TiO_2 and sulfated-TiO_2

Catalyst	$k_1(10^5)$	k_2	k_1k_2	$t_{1/2}$ (min)
TiO_2-600 °C	2.06	2772	0.057	30.4
TiO_2-SO_4-600 °C	1.99	5617	0.111	15.5

The values of $t_{1/2}$ were estimated from the data illustrated on Figs. 7 and 8 and tabulated on Table 2. The activity ($t_{1/2}$) for the TiO_2 was 30.4 min. Meanwhile, for the sulfated catalyst the activity was 15.5 min. These results show that the sulfate has a large effect in the photocatalytic decomposition of 2,4-dinitroaniline. Enhanced photoactivity by sulfuric acid treatment of TiO_2 gels has also been recently reported [57,58].

4. Discussion

The BET specific surface areas of both TiO_2 and sulfated TiO_2 samples are comparable, we can then rule out a possible surface area effect when comparing their physical and activity properties.

Pure TiO_2 with large crystallite sizes is stoichiometric, dielectric and not useful in catalysis. However, its electronic and catalytic properties change when it is doped with other atoms, when oxygen vacancies are created, or when the Ti:O stochiometry is altered. Their electronic properties depend on the local defect density and or in the type of impurities introduced. The determination of semiconductivity (E_g) of TiO_2 (3.32 eV) and sulfated TiO_2 (3.03 eV) shows that in the sulfated sample the local density has been altered if compared with TiO_2 sol–gel prepared reference. In the sulfated TiO_2 we can then expect a bigger photoactivity since its E_g is lower than that of TiO_2 reference sample. The photoefficiency depends of both of the energy required to excite the electrons from the valence band to the conductivity band (E_g) and of the electron-hole pair recombination [1]. In our opinion a combined effect, electron trap species, which diminishes the rate of electron pair recombination, and a lowest E_g seems operate in the sulfated TiO_2 as it is discussed later.

It has been reported that transition metals supported on TiO_2 play the role of electron traps improving the oxidation process, since the re-combination of holes and electrons induced by UV irradiation is avoided (14,15). In sulfated-titania the O=S=O anchored to the surface seems to play a similar role. The O=S=O species in water polarized the S=O bonds to coordinate water, giving an anchored sulfate, in which a sulfur electron deficient species is induced. In Fig. 9, the model by which this polarization occurs is shown.

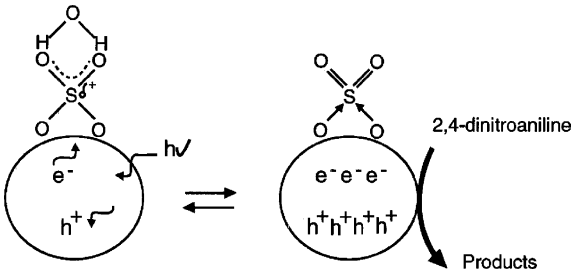

Fig. 9. Model explaining the role of sulfate on sulfated-TiO_2 photoactivity.

The role of the acidity determined by means of FTIR-pyridine adsorption studies in the photoactivity is unclear. The photoactivity of the sulfated TiO_2 was determined in aqueous media and the pyridine adsorption in vacuum. However, from pyridine adsorption FTIR spectra, we observe that strong acidity is developed in such sample, and therefore its use can be extrapolated to acid–basic heterogeneous reactions in a near future. In the present work, following the shift of the band from 1266 to 1331 cm^{-1} when pyridine was desorbed, we can speculate that similar effect occurs with the evolution of coordinated water to S–O^- bonds, if we assume that pyridinic ion is adsorbed in similar way as that proposed for coordinated water in Fig. 3. Pyridine adsorption then, is used in this paper as an indirect determination of water S–O^- coordination.

A correlation between the titania phases and the photoactivity has been reported [5,7]. In our sol–gel sulfated-titania this assumption can be taken into account, since the higher activity corresponds to sulfated-TiO_2, catalyst in which anatase is the only crystalline phase observed. On the other hand, it has also been reported that the acidity of the reactant medium favors the photoactivity [4]. To analyze the possible effect of pH on the activity, TiO_2 and the sulfated-titania (200 mg) calcined at 600 °C were put in 20 ml of water under stirring, and after 3 h the pH of the filtered solution was determined. In both cases

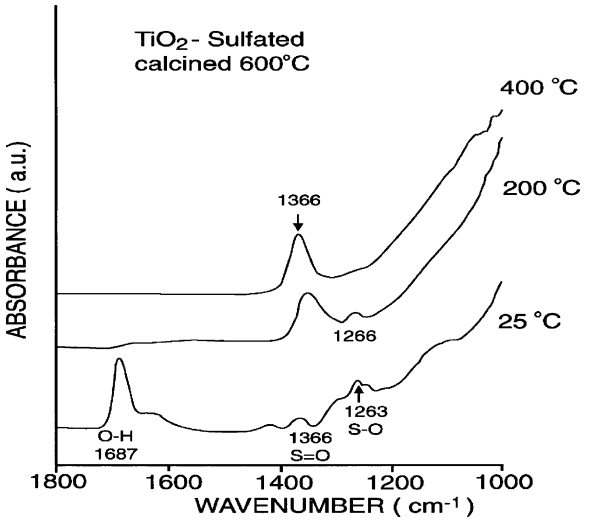

Fig. 10. FTIR spectra of "used" sulfated-TiO_2 (600 °C) catalyst.

the pH of the solution was constant (pH 6.7). Additionally, after the decomposition of the 2,4-dinitroaniline, the used sulfated-titania was filtered and after drying at 110 °C, the S=O bond was identified by FTIR-spectroscopy. In Fig. 10, the S=O vibration band at 1366 cm^{-1} is observed in situ even after heating the used sample to 400 °C, indicating that the S=O species remained in used catalysts. The probable mechanism by which the SO_4^{2-} ion is strongly anchored to TiO_2 may be similar to that proposed in SiO_2–ZrO_2 sol–gel mixed oxides [59], where the S–O^- bonds replace the vacancies formed during the dehydroxylation of the TiO_2 gel. Note that the sulfation was made on gelled and dried TiO_2 (fresh sample) and then over a highly hydroxylated TiO_2 [60].

In other words, we can say that the sulfate anchored on the titania surface is helpful in the transfer and separation of photogenerated electrons and holes. The polarization of S=O bonds by coordinated water plays and essential role in the highest photoactivity of sulfated TiO_2.

5. Conclusions

The main conclusions of the present work are the following: (i) O=S=O bonds were identified in sulfated samples; (ii) FTIR-pyridine absorption spectra show the formation of Bronsted and Lewis sites in sulfated-titania; (iii) the activity of the sulfated-titania in the decomposition of 2,4-dinitroaniline is higher on sulfated-TiO_2 than on TiO_2; (iv) a model in which the sulfate anchored to the titania surface, acquires an electron deficient character and acts as an electron trap is proposed to explain the activity of the sulfated-titania.

Acknowledgements

We are indebted to CONACYT for financial support.

References

[1] J.E. Hermann, Catal. Today 53 (1999) 115.
[2] M.I. Litter, Appl. Catal. B: Environ. 23 (1999) 89.
[3] I. Arslan, I.A. Blacioglu, D.W. Bahnemman, Appl. Catal. B: Environ. 26 (2000) 193.
[4] K.H. Wang, Y.H. Hsieh, M.Y. Chou, C.Y. Chang, Appl. Catal. B: Environ. 21 (1999) 1.
[5] A.J. Maira, K.L. Yeung, C.Y. Lee, P.L. Yue, C.K. Chang, J. Catal. 192 (2000) 185.
[6] D. Chen, A.K. Ray, Appl. Catal. B: Environ. 23 (1999) 143.
[7] S.J. Tsai, S. Cheng, Catal. Today 33 (1997) 227.
[8] V. Loddo, G. Marci, L. Palmisano, A. Sclafani, Mater. Chem. Phys. 53 (1988) 217.
[9] V. Loddo, G. Marci, C. Martin, L. Palmisano, V. Rives, A. Sclafani, Appl. Catal. B: Environ. 20 (1999) 29.
[10] I. Ilisz, Z. Laszlo, A. Dombi, Appl. Catal. A: Gen. 180 (1999) 25.
[11] V. Brezova, A. Stasko, J. Catal. 147 (1994) 156.
[12] D.S. Muggly, J.T. McCue, J.L. Falconer, J. Catal. 173 (1998) 470.
[13] D.V. Kozlov, E.A. Paukshtis, E.N. Savinov, Appl. Catal. B: Environ. 23 (2000) L7.
[14] J.M. Hermann, H. Tahiri, Y. Ait-Ichou, G. Lassaletta, A.R. Gonzalez-Elipe, A. Fernandez, Appl. Catal. B: Environ. 13 (1997) 219.
[15] A. Sclafini, J.M. Hermann, Phtochem. Photobiol. A: Chem. 113 (1998) 181.
[16] A. Blazkova, I. Csolleova, V. Brezova, Photochem. Photobiol. A: Chem. 113 (1988) 251.
[17] A. Linsebigler, C. Rusu, J.T. Taylor, J. Am. Chem. Soc. 118 (1996) 5284.
[18] J. Taguchi, T. Okuhara, Appl. Catal. A: Gen. 194/195 (2000) 89.
[19] S.M. Junge, P. Grange, Catal. Today 59 (2000) 305.
[20] R.T. Yang, W.B. Li, N. Chen, Appl. Catal. A: Gen. 169 (1998) 215.
[21] A.K. Dalai, R. Sethuraman, S.P.R. Katikanemi, R.O. Idem, Ind. Eng. Chem. Res. 37 (1998) 3869.

[22] H. Kominami, J. Kato, Y. Takada, Y. Doushi, B. Ohtani, S. Nishimoto, M. Inoue, T. Inui, Y. Kera, Catal. Lett. 46 (1997) 235.
[23] T.J. Bastow, H.J. Whifield, Chem. Mater. 11 (1999) 3518.
[24] K.Y. Jung, S.B. Park, Appl. Catal. B: Environ. 25 (2000) 249.
[25] H. Kominami, J. Kato, S. Murakami, Y. Kera, M. Inoue, T. Inue, B.J. Ohtani, J. Mol. Catal. 144 (1999) 165.
[26] G. Facchin, G. Carturan, R. Campostrini, S. Gialanella, L. Lutterotti, L. Armelao, G. Marci, L. Palmisano, A. Sclafani, J. Sol–Gel Sci. Technol. 18 (2000) 29.
[27] J.A. Navio, G. Colon, M. Macias, C. Real, M.I. Litter, Appl. Catal. A: Gen. 177 (1999) 111.
[28] J.A. Navio, J.J. Testa, P. Djedjeian, J.R. Padron, D. Rodriguez, M.I. Litter, Appl. Catal. A: Gen. 178 (1999) 191.
[29] G.P. Lepore, L. Persau, C.H. Langford, J. Photochem. Photobiol. 98 (1996) 103.
[30] M.E. Zorn, D.T. Tompkins, W.A. Zeltner, M.A. Anderson, Appl. Catal B: Environ. 23 (1999) 1.
[31] X. Fu, W.A. Zeltner, Q. Yang, M.A. Anderson, Catalysis 168 (1997) 482.
[32] Y. Hiang, B. Zhao, Y. Xie, Appl. Catal. A: Gen. 171 (1988) 65.
[33] J. Navarrete, T. López, R. Gómez, F. Figueras, Langmuir 12 (1996) 4385.
[34] X. Bokhimi, A. Morales, O. Novaro, T. López, E. Sánchez, R. Gómez, J. Mater. Res. 10 (1995) 2778.
[35] E. Sánchez, T. López, R. Gómez, X. Bokhimi, A. Morales, O. Novaro, J. Solid State Chem. 122 (1996) 309.
[36] X. Bokhimi, O. Novaro, R.D. Gonzalez, T. López, O. Chimal, M. Asomoza, R. Gómez, J. Solid State Chem. 144 (1999) 349.
[37] E. Sánchez, T. López, Mater. Lett. 25 (1995) 271.
[38] T. López, R. Gómez, G. Pecchi, P. Reyes, X. Bokhimi, O. Novaro, Mater. Lett. 40 (1999) 59.
[39] T. López, E. Sánchez, R. Gómez, L. Ioffe, Y. Borodko, React. Kinet. Catal. Lett. 61 (1997) 289.
[40] T. López, R. Gómez, E. Romero, I. Schifter, React. Kinet. Catal. Lett. 49 (1993) 95.
[41] S. Castillo, M. Moran-Pineda, R. Gómez, J. Catal. 172 (1997) 263.
[42] R. Gómez, T. López, S. Castillo, R.D. Gonzalez, J. Sol–Gel Sci. Technol. 1 (1994) 205.
[43] S. Castillo, M. Moran-Pineda, V. Molina, R. Gómez, T. López, Appl. Catal. B: Environ. 15 (1998) 203.
[44] R.D. Gonzalez, T. López, R. Gómez, Catal. Today 35 (1997) 293.
[45] T. López, R. Gómez, in: Sol–Gel Optics, L.C. Klein (Ed.), Kluwer Academic Publishers, Northweel, MA, USA, 1994, p. 345.
[46] P. Thomson, D.E. Cox, J.B. Hastings, J. Appl. Crystallogr. 20 (1994) 79.
[47] R.A. Young, P. Desai, Arch. Nauki Mater. 10 (1989) 71.
[48] O. Saur, M. Bensitel, A.B. Mohammed, J.C. Lavalley, J. Catal. 99 (1986) 104.
[49] A.B. Da Silva, E. Jordao, M.J. Mendes, P. Fouilloux, Appl. Catal. A: Gen. 148 (1997) 253.
[50] T. Yamaguchi, Appl. Catal. 61 (1990) 1.
[51] M. Bensitel, O. Saur, J.C. Lavalley, B.A. Manrov, Mater. Chem. Phys. 19 (1998) 147.
[52] T. Yamaguchi, J. Tuo, K. Tanabe, J. Phys. Chem. 90 (1986) 3148.
[53] A.L. Linsebigier, G. Lu, J.T. Yates Jr., Chem. Rev. 95 (1995) 735.
[54] C. Monterra, G. Cerrato, V. Bolis, Catal. Today 17 (1993) 505.
[55] N. Serpone, E. Pellizetti, Photocatalysis Fundamental and Applications, Wiley, New York, 1989.
[56] T. López, J. Hernández-Ventura, R. Gómez, F. Tzompantzi, E. Sánchez, X. Bokhimi, A. García, J. Mol. Catal. A: Chem. 167 (2001) 101.
[57] J.C. Yu, J. Yu, J. Zhao, Appl. Catal. B: Environ. 36 (2002) 31.
[58] S. Yanazaki, N. Fujinaga, K. Araki, Appl. Catal. A: Gen. 210 (2001) 97.
[59] T. López, F. Tzompantzi, J. Navarete, R. Gómez, J.L. Boldu, E. Muñoz, O. Novaro, J. Catal. 181 (1999) 285.
[60] T. López, E. Sánchez, P. Bosch, Y. Meas, R. Gómez, Mater. Chem. Phys. 32 (1992) 141.